arXiv:1402.3082v2 [cond-mat.str-el] 24 Apr 2014

Unusual spin fluctuations and magnetic frustration in olivine and non-olivine $LiCoPO_4$ detected by ^{31}P and ^{7}Li nuclear magnetic resonance

S.-H. Baek,[1,*] R. Klingeler,[2] C. Neef,[2] C. Koo,[2] B. Büchner,[1,3] and H.-J. Grafe[1]

[1] *IFW-Dresden, Institute for Solid State Research, PF 270116, 01171 Dresden, Germany*
[2] *Kirchhoff Institute for Physics, University of Heidelberg, 69120 Heidelberg, Germany*
[3] *Institut für Festkörperphysik, Technische Universität Dresden, 01062 Dresden, Germany*

(Dated: April 25, 2014)

We report ^{31}P and ^{7}Li nuclear magnetic resonance (NMR) studies in new non-olivine $LiZnPO_4$-type $LiCoPO_4^{tetra}$ microcrystals, where the Co^{2+} ions are tetrahedrally coordinated. Olivine $LiCoPO_4$, which was directly transformed from $LiCoPO_4^{tetra}$ by an annealing process, was also studied and compared. The uniform bulk magnetic susceptibility and the ^{31}P Knight shift obey the Curie-Weiss law for both materials with a high spin Co^{2+} ($3d^7$, $S = 3/2$), but the Weiss temperature Θ and the effective magnetic moment $\mu_{\rm eff}$ are considerably smaller in $LiCoPO_4^{tetra}$. The spin-lattice relaxation rate T_1^{-1} reveals a quite different nature of the spin dynamics in the paramagnetic state of both materials. Our NMR results imply that strong geometrical spin frustration occurs in tetrahedrally coordinated $LiCoPO_4$, which may lead to the incommensurate magnetic ordering.

I. INTRODUCTION

The olivine structured lithium transition metal phosphates $LiMPO_4$ (M = Fe, Mn, Co, and Ni) have attracted interest from both fundamental and technical points of view. They reveal a variety of unusual magnetic, magnetoelectric, and ferrotoroidic properties associated with high spin (HS) M^{2+} ions.[1–5] Also, their low cost, low toxicity, high stability, and high energy density made them promising candidates of high-voltage cathode materials for Li-ion batteries.[6–11] Among the olivine $LiMPO_4$ family, $LiCoPO_4$ features a very large linear magnetoelectric effect[12,13] and a high theoretical energy density up to 801 Wh/kg based on its high discharge plateau 4.8 V versus Li/Li^+.[14,15]

Olivine $LiCoPO_4$ crystallizes in the orthorhombic $Pnma$ space group.[16] The Co^{2+} ($S = 3/2$) ions sit in the center of the distorted CoO_6 octahedra which share corners and edges with PO_4 tetrahedra, as illustrated in Fig. 1(a). Below $T_N \sim 21$ K, the moments order antiferromagnetically, with a tilt of 4.6° away from the crystallographic b axis within the bc plane, and the crystal structure changes to the $P12'_11$ symmetry.[17–19] In this low symmetry, a nonzero toroidal moment is allowed and confirmed experimentally.[2,20]

For optimal performance of electrode materials for Li-ion batteries, it is crucial to get insight into the fundamental structural, electronic, and magnetic properties of the materials and their limits and trends for applications.[21] Therefore, recently discovered non-olivine structured $LiCoPO_4$ is interesting and may provide an important step forward in the understanding of the impact of structure and magnetism on the performance of a battery material. $LiCoPO_4^{tetra}$ possesses $Pn2_1a$ symmetry and consists of CoO_4 tetrahedra, instead of CoO_6 octahedra in the olivine structure, sharing only corners with PO_4 tetrahedra[22,23] [see Fig. 1(b)]. The non-olivine structure becomes unstable at high temperatures towards the olivine one.

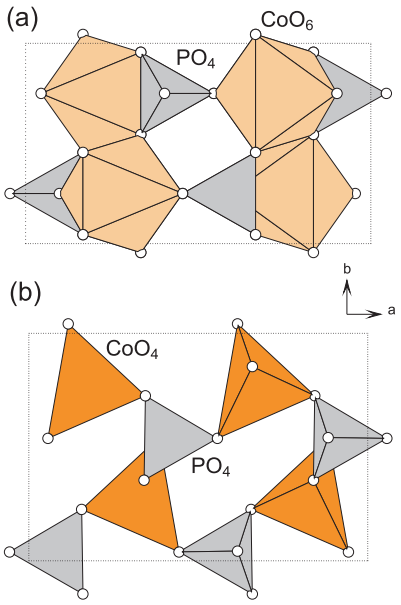

FIG. 1: (Color online) Crystal structure of (a) olivine ($Pnma$ symmetry) and (b) tetrahedral ($Pn2_1a$ symmetry) $LiCoPO_4$, projected along the crystallographic c axis. Li atoms are omitted for clarity. Their unit cells are drawn as dotted lines.

Initial studies indicate that tetrahedral $LiCoPO_4$ exhibits poor performance in terms of cycling stability and discharge capacity compared to the olivine phosphate.[23] In an attempt to elucidate the detailed magnetic properties of both compounds associated with their structural aspects, we carried out an NMR study on tetrahedral $LiCoPO_4^{tetra}$ as well as on the annealed olivine compound. Our results of the Knight shift and the spin-lattice relaxation rates show that the tetrahedrally coordinated Co^{2+} spins in $LiCoPO_4^{tetra}$ are strongly frustrated, resulting in quite different magnetic properties, compared to olivine

$LiCoPO_4$. The magnetic structure in the ordered state is likely incommensurate.

II. SAMPLE PREPARATION AND EXPERIMENTAL DETAILS

Non-olivine $LiCoPO_4^{tetra}$ microcrystals with $Pn2_1a$ symmetry were synthesized by the microwave-assisted hydrothermal synthesis technique, as described in detail in Refs. 23,24. Olivine $LiCoPO_4$ with $Pnma$ symmetry was obtained by annealing the non-olivine compound at 700°C for 24 hours under an argon atmosphere.

The temperature dependence of the static uniform magnetic susceptibility $\chi(0,0)$ of $LiCoPO_4^{tetra}$ and $LiCoPO_4^{olivine}$ was measured using a superconducting quantum interference device (SQUID) magnetometer in the field of 1 kOe after cooling in zero magnetic field.

^{7}Li and ^{31}P NMR measurements have been carried out using a spin-echo method in a fixed field of 7.0494 T in the temperature range of 5–400 K. Since ^{31}P (nuclear spin $I = 1/2$, $\gamma_n = 17.2356$ MHz/T) does not involve electric quadrupole effects, it is an ideal probe to study magnetism and spin fluctuations in these materials. ^{31}P NMR spectra over most of the measured temperature range are relatively narrow and quite symmetric, in comparison with the large linewidth and strong anisotropy observed in other Li phosphates,[25,26] which allowed us to determine the Knight shift and the linewidth reliably. The spin-lattice relaxation rates T_1^{-1} of both ^{31}P and ^{7}Li ($I = 3/2$, $\gamma_n = 16.5471$ MHz/T) were measured using the saturation recovery method and T_1 was obtained by fitting the relaxation of the nuclear magnetization $M(t)$ to a single exponential function, $1-M(t)/M(\infty) = A\exp(-t/T_1)$ where A is a fitting parameter.

III. EXPERIMENTAL RESULTS AND DISCUSSION

A. Magnetic susceptibility χ and ^{31}P Knight shift $\mathcal{K}$

Figure 2 shows the molar static susceptibility $\chi_{mol} = M/H$ as a function of temperature for both olivine and tetrahedral $LiCoPO_4$. The drop of the χ data at low temperatures indicates that in both systems long range antiferromagnetic order evolves at low temperature. The transition can be clearly observed in the magnetic specific heat $c_{mag} \sim \partial(\chi_{mol}T)/\partial T$ (see inset) as both compounds show an anomaly at $T_N = 21$ and 7 K, respectively.

At high temperatures, the data in both compounds follow a Curie-Weiss (CW) law, $\chi_{mol} = C/(T+\Theta) + \chi_0$, where χ_0 is a T-independent susceptibility [see inset of Fig. 2(b)]. Fitting the data with the CW law yields the Weiss temperatures $\Theta = 52(5)$ K (olivine) and $\Theta = 7(1)$ K (tetra), and the effective magnetic moments $\mu_{eff} = 5.1\mu_B$ (olivine) and $4.4\mu_B$ (tetra). Both values of μ_{eff} exceed the spin-only value of 3.87 μ_B expected

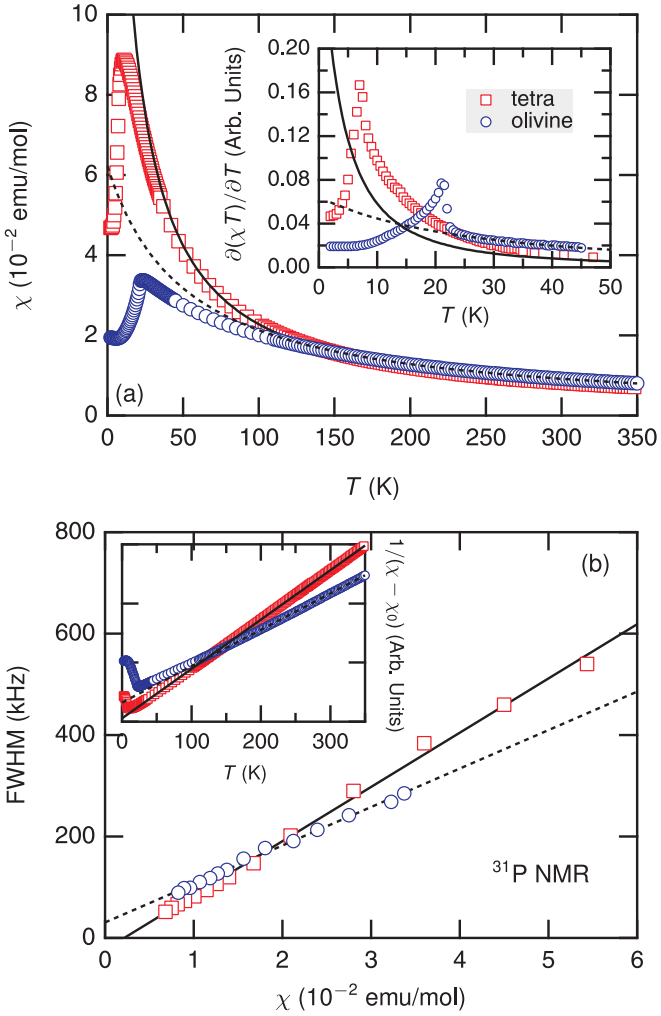

FIG. 2: (Color online)(a) Temperature dependence of static susceptibility and magnetic specific heat (inset) of both olivine and tetrahedral $LiCoPO_4$. Solid curves are Curie-Weiss fits. (b) NMR linewidth (FWHM) of ^{31}P spectrum (see Fig. 3) tracks χ in the whole temperature range investigated. Inset: Inverse static susceptibility.

for the HS $3d^7$ configuration for full quenching of the orbital moment. In $LiCoPO_4^{tetra}$, the orbital admixture to the measured effective $g = 2.27$ is governed by the reduced spin-orbit coupling λ and the tetrahedral crystal field (CF) splitting Δ_t of the Co^{2+} orbital states of e_g and t_{2g} symmetry. It can be approximated by

$$g = 2 - \frac{8\cdot\lambda}{\Delta_t}. \qquad (1)$$

With $\lambda \approx -143$ cm^{-1},[27] the data are consistent with $\Delta_t \approx 4250$ cm^{-1}. In contrast, the electronic configuration of HS Co^{2+} in the octahedral configuration $t_{2g}^5 e_g^2$ realized in $LiCoPO_4^{olivine}$ exhibits a stronger orbital contribution since it involves only partially filled low-lying orbital triplet states with pseudo angular momentum $\tilde{l} = 1$.

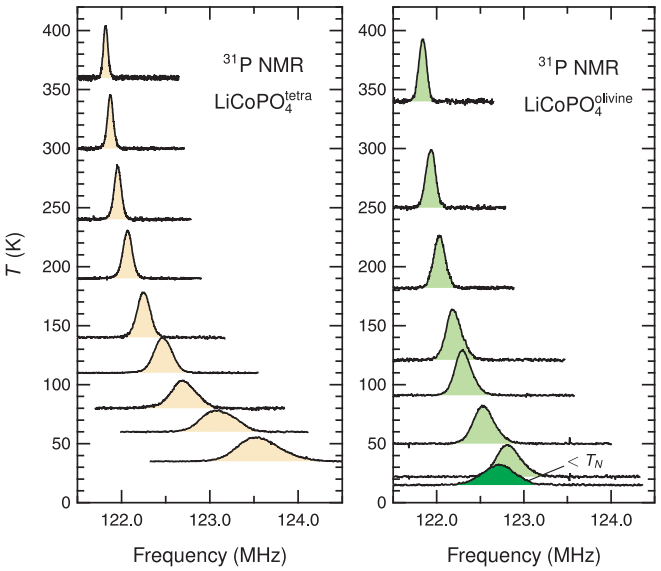

FIG. 3: (Color online) Temperature evolution of ^{31}P NMR spectrum obtained at 7.0494 T for both tetrahedral (left) and olivine (right) $LiCoPO_4$ in the paramagnetic state. The spectrum in the ordered state for $LiCoPO_4^{olivine}$ is also shown for comparison.

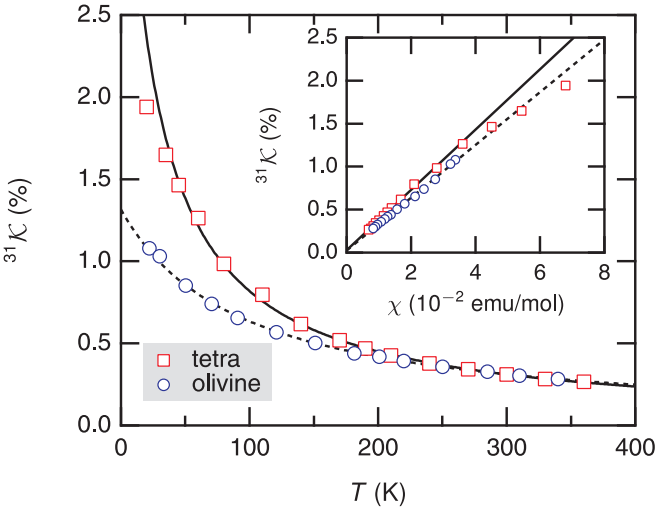

FIG. 4: (Color online) The ^{31}P Knight shift as a function of temperature. Solid curves are Curie-Weiss fits. The inset shows a plot of $\mathcal{K}(T)$ versus $\chi(0,0)(T)$ with T as implicit parameter. The slope of the data yields the hyperfine coupling constants $A_{\rm hf} = 1.96$ kOe/μ_B and 1.71 kOe/μ_B for $LiCoPO_4^{tetra}$ and $LiCoPO_4^{olivine}$, respectively. The T-independent orbital shifts are found to be nearly zero (see text).

The observed effective moment agrees well with the findings in Ref. 18.

In this paper, we mainly concentrate on the NMR data obtained on both materials. Hence, we note that the broadening of the NMR line is essentially determined by the uniform bulk susceptibility as can be deduced from Fig. 2 (b) where the full width at half maximum (FWHM) of the ^{31}P NMR spectra is plotted against χ with T as an implicit parameter. Further information on the static magnetic properties is obtained from measurements of the ^{31}P Knight shift, $^{31}\mathcal{K}$. Its temperature dependence confirms CW-behavior in both materials. The data in Fig. 4 are well described by $\mathcal{K} = C'/(T+\Theta)+\mathcal{K}_0$, where $\mathcal{K}_0$ is the T-independent orbital shift. For both materials, $\mathcal{K}_0$ appears negligibly small, indicating that $\mathcal{K}$ probes almost entirely the spin part of the magnetic susceptibility.

Focusing on the evolution of antiferromagnetic order, the static susceptibility data imply deviations from the mean-field Curie-Weiss-like behavior already at relatively high temperatures. In the olivine sample, small deviations from the experimental data are observed below ~ 250 K as visible in Figs. 2(a) and (b, inset). The experimentally observed susceptibility is smaller than predicted by the Curie-Weiss law which is in agreement with the evolution of antiferromagnetic fluctuations well above T_N. In the tetragonal polymorph, such behavior is present below ~ 50 K which is best seen if the magnetic specific heat in Fig. 2 (a) (inset) is considered.

In order to compare the static susceptibility measured by bulk and local techniques, the inset of Fig. 4 shows a plot of $^{31}\mathcal{K}$ versus χ. $^{31}\mathcal{K}$ is proportional to χ over a wide temperature range. The small deviation from linearity occurring below ~ 60 K for $LiCoPO_4^{tetra}$ is attributed to a small amount of paramagnetic (PM) impurities to which $\mathcal{K}$ is insensitive. This account is indeed corroborated by the good agreement between the linewidth and χ in the T region where $\mathcal{K}$ deviates χ, as shown in the inset of Fig. 2, since a random distribution of PM moments would broaden the NMR line without affecting its shift.

The linear slope of $d\mathcal{K}/d\chi$ corresponds to the hyperfine (hf) coupling constants, $A_{\rm hf} = 1.96$ kOe/μ_B (tetra) and 1.71 kOe/μ_B (olivine). Note that $^{31}\mathcal{K}$ in both compounds almost vanishes at $\chi = \chi_0 \sim 0$, confirming the non-spin susceptibility contribution $\mathcal{K}_0 \sim 0$.

B. Spin-lattice relaxation rate T_1^{-1} and dynamical susceptibility

The ^{31}P spin-lattice relaxation rate $^{31}T_1^{-1}$ as a function of temperature is presented in Fig. 5. For the olivine compound, $^{31}T_1^{-1}$ increases steadily with decreasing T and is rapidly enhanced below 40 K, exhibiting a sharp anomaly followed by a rapid drop. The sharp peak (vertical solid line) indicates the onset of magnetic order at $T_N = 21$ K, which agrees with literature values.[16,18,19] The rapid upturn above T_N, which is due to the critical slowing down of spin fluctuations towards magnetic order, is a rough measure of dimensionality of the magnetic system as well. In our case, the relatively sharp transition width which is comparable to T_N indicates the quasi-three-dimensional nature of the magnetic order

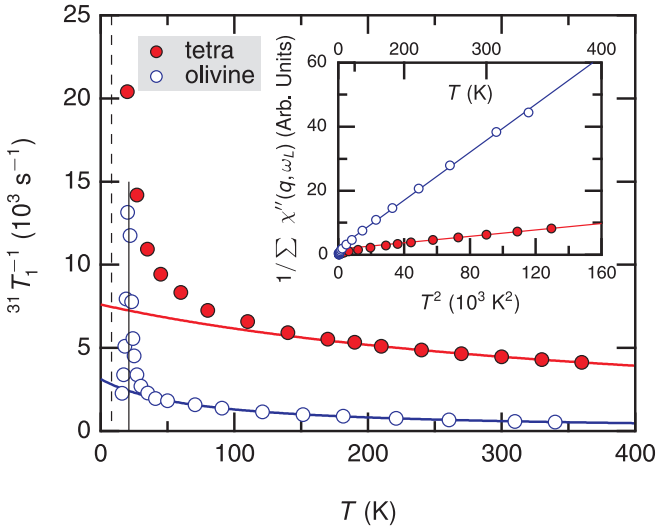

FIG. 5: (Color online) ^{31}P spin-lattice relaxation rate $^{31}T_1^{-1}$ as a function of temperature in olivine and tetrahedral $LiCoPO_4$ samples. For $LiCoPO_4^{olivine}$, $^{31}T_1^{-1}$ reveals a sharp magnetic transition at $T_N = 21$ K (vertical solid line), while it diverges towards $T_N = 7$ K (vertical dashed line) for $LiCoPO_4^{tetra}$. Solid curves are equivalent to the linear fit in Fig. 7. The inset presents a plot of $1/\sum_q \chi''(q,\omega_L)$ versus T^2, to show the inverse dynamical susceptibility that is quadratic in temperature.

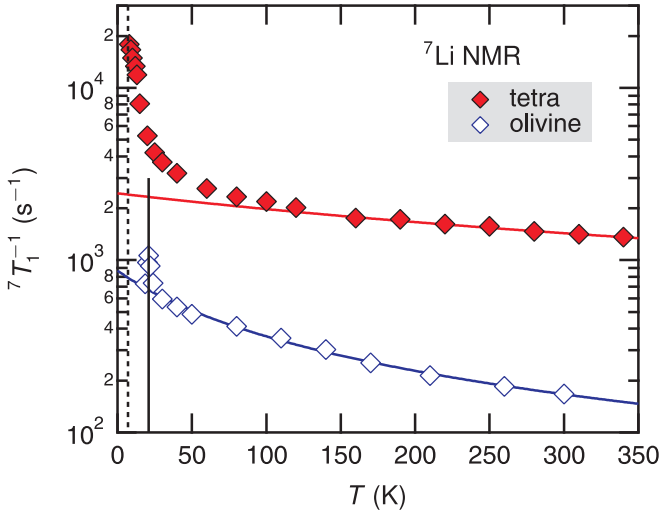

FIG. 6: (Color online) Temperature dependence of the ^{7}Li spin-lattice relaxation rate. Data in the PM region resemble those of $^{31}T_1^{-1}$, indicating that both ^{7}Li and ^{31}P nuclei are governed by the same relaxation mechanism. The solid curves are identical with those in Fig. 5 with scaling. A sharp anomaly was detected at $T_N = 21$ K for $LiCoPO_4^{olivine}$, similar to the case of ^{31}P.

rather than two-dimensional (2D).[18,28] For $LiCoPO_4^{tetra}$, the $^{31}T_1^{-1}$ data are an order of magnitude larger than those of $LiCoPO_4^{olivine}$, displaying a similar temperature dependence. T_N could not be identified since $^{31}T_1$ becomes too short to be measured near the transition, but the temperature at which $^{31}T_1^{-1}$ diverges appears to be consistent with $T_N = 7$ K (vertical dashed line).

For olivine $LiCoPO_4$, inelastic neutron scattering yields moderate magnetic exchange coupling constants.[29] In the *bc*-plane, the dominating nearest neighbor coupling amounts to $J_{\parallel}^{nn} = 9\,\mathrm{K}$ while smaller next nearest neighbor and interlayer couplings of $\sim 1 - 2\,\mathrm{K}$ imply a tendency to weak frustration and 2D behavior. In the case of $LiCoPO_4^{tetra}$, where T_N as well as Θ are significantly smaller than in the olivine material, magnetic coupling is presumingly weaker and/or the tendency towards 2D and frustration stronger.

In the paramagnetic limit, T_1^{-1} could be approximated by the relation,[30]

$$T_1^{-1} \propto \frac{A_{\mathrm{hf}}^2 \sqrt{S(S+1)}}{\hbar J_{\mathrm{ex}}}. \qquad (2)$$

Using this equation, one can estimate the ratio, $T_1^{-1}(\mathrm{tetra})/T_1^{-1}(\mathrm{olivine}) = 6.5$, using the relation $J_{\mathrm{ex}} \equiv 3k_B\Theta/[zS(S+1)]$ where z is the number of nearest-neighbors. This value satisfactorily accounts for the difference of $^{31}T_1^{-1}$ between the two compounds at high temperatures, proving that the system indeed lies in the localized limit at high temperatures.

In general, while the Knight shift is proportional to the static spin susceptibility at $q = 0$, i.e. $\mathcal{K} = A_{\mathrm{hf}}\chi(0,0)$, T_1^{-1} reflects the q-average of the imaginary part of the dynamical susceptibility χ'' at low energy,[31]

$$T_1^{-1} \propto T\gamma_n^2 A_{\mathrm{hf}}^2 \sum_q \chi''(q,\omega_L)/\omega_L, \qquad (3)$$

where γ_n is the nuclear gyromagnetic ratio and ω_L the Larmor frequency. Since there is no difference of the Knight shift at high temperatures far above T_N between the two compounds, we conclude that spin fluctuations are of dominantly antiferromagnetic nature for both olivine and tetrahedral $LiCoPO_4$.

The most striking feature is that $^{31}T_1^{-1}$ for both compounds increases with decreasing temperature, as shown in Fig. 5. Such a $1/T$ dependence of T_1^{-1} is very rare in the paramagnetic limit. Figure 7 clearly shows the linear variation of T_1 in terms of T, particularly, in $LiCoPO_4^{olivine}$. This in turn implies that the q-average of the dynamical susceptibility $\sum_q \chi''(q,\omega_L)$ from Eq. (3) varies in proportion to $1/T^2$, in contrast to the uniform static susceptibility $\chi(0,0)$ that obeys the CW law. A plot of $1/\sum_q \chi''(q,\omega_L)$ versus T^2 is given in the inset of Fig. 5, which provides evidence of the quadratic temperature dependence of the inverse dynamical susceptibility. Note that this plot eliminates the effect of the hf coupling constants, allowing the direct comparison of the two systems.

To ensure that the unusual T dependence of $^{31}T_1^{-1}$ is not site dependent, but represents the intrinsic dynamical susceptibility of the system, we also measured the ^{7}Li spin-lattice relaxation rate, $^7T_1^{-1}$, as a function of tem-

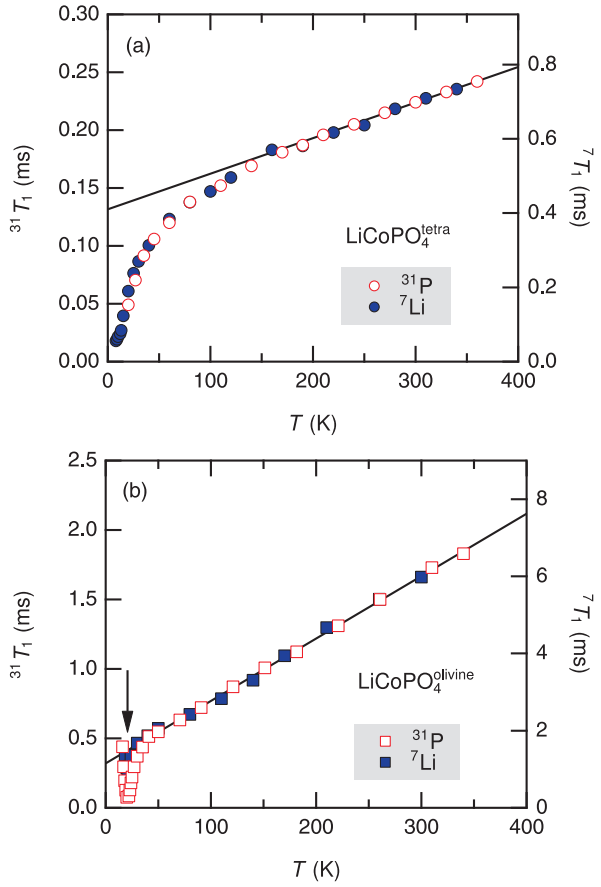

FIG. 7: (Color online) For (a) $LiCoPO_4^{tetra}$ and (b) $LiCoPO_4^{olivine}$, the spin-lattice relaxation times $^{31}T_1$ and $^{7}T_1$ as a function of temperature are scaled to each other, demonstrating that they detect the dynamical susceptibility $\sum_q \chi''(q,\omega_L)$ of the materials. While the linear T dependence of T_1 is well maintained over the whole temperature range investigated, except near the transition at T_N for $LiCoPO_4^{olivine}$, it breaks down below $\sim$ 150 K for $LiCoPO_4^{tetra}$.

perature. The results are presented in Fig. 6, revealing a T dependence similar to $^{31}T_1^{-1}$. In fact, Fig. 7 proves that $^{31}T_1$ and $^{7}T_1$ as a function of temperature are accurately scaled to each other for both compounds.[34]

From Figs. 5 and 7, the different behaviors of T_1^{-1} in the two compounds are noticeable. Namely, for $LiCoPO_4^{olivine}$, the T_1 data follow a linear T behavior in the whole temperature range investigated except the region near $T_N^{olivine}$. In contrast, for $LiCoPO_4^{tetra}$, the T_1 data deviate from the T-linear behavior at $\sim$ 150 K, suggesting that an additional relaxation mechanism is developed. Another noticeable feature is that the T-linearity of T_1 is considerably smaller in $LiCoPO_4^{tetra}$, seemingly approaching the normal CW behavior [i.e., $T_1(T) \rightarrow$ constant at high T] which is observed in other olivine lithium phosphates, $LiMnPO_4$ and $LiFePO_4$.[25]

The different magnetic properties of $LiCoPO_4^{tetra}$ and $LiCoPO_4^{olivine}$ could be understood by considering their inherent spin networks. There are five exchange pathways between the Co^{2+} spins in olivine $LiCoPO_4$.[29,32] In the bc plane, one can identify the nearest-neighbor coupling J_1 mediated through Co-O-Co superexchange path and the next-nearest-neighbor coupling J_2 and J_3 along the b and c axes, respectively, through PO_4 tetrahedra [Fig. 1(a) depicts only J_1 coupled Co atoms]. The interplane couplings J_4 and J_5 are also mediated by PO_4 tetrahedra and are known to be ferromagnetic, while the intraplane couplings J_1, J_2, and J_3 are all antiferromagnetic. This spin network involves weak geometrical frustration since J_1 is much larger than other exchange couplings.[29]

This situation is dramatically altered in $LiCoPO_4^{tetra}$. As clearly shown in Fig. 1(b), there is no longer a Co-O-Co superexchange path and all the exchange interactions are mediated by corner-shared PO_4 tetrahedra and might be comparable to each other in strength. Naturally, this spin network likely results in strong frustration. The frustration may be consistent with the strong reduction of the effective exchange interaction and ordering temperature T_N. Note that in the case of competing ferromagnetic and antiferromagnetic interactions the ratio T_N/Θ does not provide reliable information on magnetic frustration. Since Co^{2+} ions behave more like paramagnets in $LiCoPO_4^{tetra}$, one may argue that the frustration effect modifies the spin dynamics which causes the peculiar upturn of T_1^{-1}. At low temperatures, the frustration can induce the incommensurate or spin-glass-like magnetic ordering. In this case, magnetic short-range fluctuations may extend far above T_N, being responsible for the additional enhancement of T_1^{-1} which was observed below $\sim$ 150 K.

Now we discuss the puzzling feature of the $1/T$-dependence of T_1^{-1}, which implies the inverse quadratic temperature dependence of the dynamical susceptibility. To begin with, one may conjecture that Li diffusion motion causes the increase of T_1^{-1} with decreasing T. However, we rule out this possibility because both mobile ^{7}Li and immobile ^{31}P nuclei detect the identical T-dependence of T_1^{-1}, as demonstrated in Fig. 7. In principle, A_{hf} may increase with decreasing T, causing the T-dependence of T_1^{-1}. Again, this is clearly not the case from the uniquely defined A_{hf} from the $\mathcal{K}$ vs. χ plot over a wide temperature range (see the inset of Fig. 4). Therefore, we conclude that unusual spin dynamics is present and persists even in the high T region ($T \gg 10J_{ex}$), causing the inverse quadratic T-dependence of $\sum_q \chi''(q,\omega_L)$. One plausible explanation could be given if J_{ex} in Eq. (2) decreases with decreasing temperature.[33] Although this scenario may be incompatible with the well-defined $\Theta \propto J_{ex}$, if spin fluctuations at small $q < Q$ are developed with decreasing temperature, the resultant effective exchange coupling could be reduced.

IV. CONCLUSIONS

We present ^{7}Li and ^{31}P NMR studies in both non-olivine and olivine structured $LiCoPO_4$ microcrystals. It turns out that the exchange interactions among the Co^{2+} spins are greatly reduced in $LiCoPO_4^{tetra}$, which accounts for the difference of the spin-lattice relaxation rates T_1^{-1} between the two compounds. In contrast to the Curie-Weiss behavior of the static susceptibility found at high temperatures, the dynamical spin susceptibility deduced from the spin-lattice relaxation rates is inversely quadratic in temperature, which is particularly strong and robust in $LiCoPO_4^{olivine}$. For $LiCoPO_4^{tetra}$, the unusual temperature dependence is considerably weakened and breaks down at low temperatures. Together with the reduced effective exchange coupling and ordering temperature, this different spin dynamics is attributed to strong frustration effect inherent in the corner-shared CoO_4-PO_4 geometry of this metastable material. The additional enhancement T_1^{-1} at low temperatures in $LiCoPO_4^{tetra}$ suggests that the frustration may lead to complex incommensurate magnetic order.

Acknowledgement

We thank Andrei Malyuk for annealing the $LiCoPO_4^{tetra}$ sample. This work was supported by the DFG (Grants No. GR3330/3-1 and No. KL1824/2-2) and by the BMBF (Project No. 03SF0397). S.B. acknowledges support by DFG Research Grant No. BA 4927/1-1.

* sbaek.fu@gmail.com

[1] D. Vaknin, J. L. Zarestky, J.-P. Rivera, and H. Schmid, Phys. Rev. Lett. **92**, 207201 (2004).
[2] B. B. Van Aken, J.-P. Rivera, H. Schmid, and M. Fiebig, Nature **449**, 702 (2007).
[3] B. B. Van Aken, J. P. Rivera, H. Schmid, and M. Fiebig, Phys. Rev. Lett. **101**, 157202 (2008).
[4] T. B. S. Jensen, N. B. Christensen, M. Kenzelmann, H. M. Rønnow, C. Niedermayer, N. H. Andersen, K. Lefmann, M. Jiménez-Ruiz, F. Demmel, J. Li, et al., Phys. Rev. B **79**, 092413 (2009).
[5] R. Toft-Petersen, N. H. Andersen, H. Li, J. Li, W. Tian, S. L. Bud'ko, T. B. S. Jensen, C. Niedermayer, M. Laver, O. Zaharko, et al., Phys. Rev. B **85**, 224415 (2012).
[6] A. K. Padhi, K. S. Nanjundaswamy, and J. B. Goodenough, J. Electrochem. Soc. **144**, 1188 (1997).
[7] S.-Y. Chung, J. T. Bloking, and Y.-M. Chiang, Nat Mater **1**, 123 (2002).
[8] C. A. J. Fisher, V. M. Hart Prieto, and M. S. Islam, Chem. Mater. **20**, 5907 (2008).
[9] N. N. Bramnik, K. Nikolowski, D. M. Trots, and H. Ehrenberg, Electrochem. Solid-State Lett. **11**, A89 (2008).
[10] B. Kang and G. Ceder, Nature **458**, 190 (2009).
[11] A. V. Murugan, T. Muraliganth, P. J. Ferreira, and A. Manthiram, Inorg. Chem. **48**, 946 (2009).
[12] J.-P. Rivera and H. Schmid, Ferroelectrics **161**, 91 (1994).
[13] I. Kornev, M. Bichurin, J.-P. Rivera, S. Gentil, H. Schmid, A. G. M. Jansen, and P. Wyder, Phys. Rev. B **62**, 12247 (2000).
[14] K. Amine, H. Yasuda, and M. Yamachi, Electrochem. Solid-State Lett. **3**, 178 (2000).
[15] S. Okada, S. Sawa, M. Egashira, J. ichi Yamaki, M. Tabuchi, H. Kageyama, T. Konishi, and A. Yoshino, J. Power Sources **9798**, 430 (2001).
[16] R. Santoro, D. Segal, and R. Newnham, J. Phys. Chem. Solids **27**, 1192 (1966).
[17] N. F. Kharchenko, Y. N. Kharchenko, R. Szymczak, M. Baran, and H. Schmid, Low Temp. Phys. **27**, 895 (2001).
[18] D. Vaknin, J. L. Zarestky, L. L. Miller, J.-P. Rivera, and H. Schmid, Phys. Rev. B **65**, 224414 (2002).
[19] A. Szewczyk, M. U. Gutowska, J. Wieckowski, A. Wisniewski, R. Puzniak, R. Diduszko, Y. Kharchenko, M. F. Kharchenko, and H. Schmid, Phys. Rev. B **84**, 104419 (2011).
[20] C. Ederer and N. A. Spaldin, Phys. Rev. B **76**, 214404 (2007).
[21] N. A. Chernova, G. M. Nolis, F. O. Omenya, H. Zhou, Z. Li, and M. S. Whittingham, J. Mater. Chem. **21**, 9865 (2011).
[22] G. Hautier, A. Jain, S. P. Ong, B. Kang, C. Moore, R. Doe, and G. Ceder, Chem. Mater. **23**, 3495 (2011).
[23] C. Jähne, C. Neef, C. Koo, H.-P. Meyer, and R. Klingeler, J. Mater. Chem. A **1**, 2856 (2013).
[24] C. Neef, C. Jähne, H.-P. Meyer, and R. Klingeler, Langmuir **29**, 8054 (2013).
[25] D. Arcon, A. Zorko, R. Dominko, and Z. Jaglici, J. Phys.: Condens. Matter **16**, 5531 (2004).
[26] C. Rudisch, H.-J. Grafe, J. Geck, S. Partzsch, M. v. Zimmermann, N. Wizent, R. Klingeler, and B. Büchner, Phys. Rev. B **88**, 054303 (2013).
[27] P. Sati, R. Hayn, R. Kuzian, S. Régnier, S. Schäfer, A. Stepanov, C. Morhain, C. Deparis, M. Laügt, M. Goiran, et al., Phys. Rev. Lett. **96**, 017203 (2006).
[28] P. J. Baker, I. Franke, F. L. Pratt, T. Lancaster, D. Prabhakaran, W. Hayes, and S. J. Blundell, Phys. Rev. B **84**, 174403 (2011).
[29] W. Tian, J. Li, J. W. Lynn, J. L. Zarestky, and D. Vaknin, Phys. Rev. B **78**, 184429 (2008).
[30] T. Moriya, Prog. Theor. Phys. **16**, 641 (1956).
[31] T. Moriya, J. Phys. Soc. Jpn. **18**, 516 (1963).
[32] D. Dai, M.-H. Whangbo, H.-J. Koo, X. Rocquefelte, S. Jobic, and A. Villesuzanne, Inorg. Chem. **44**, 2407 (2005).
[33] S.-H. Baek, H. Sakai, H. Lee, Z. Fisk, E. D. Bauer, and J. D. Thompson, Phys. Rev. B **82**, 035203 (2010).
[34] From the scaling, one can deduce the hf coupling constants of ^{7}Li directly from those of ^{31}P ; 0.79 kOe/μ_B (tetra) and 0.69 kOe/μ_B (olivine).